# A tunable double negative device consisting of a plasma array and a negative-permeability metamaterial

Cite as: Phys. Plasmas **27**, 023511 (2020); https://doi.org/10.1063/1.5112077
Submitted: 02 June 2019 . Accepted: 01 January 2020 . Published Online: 06 February 2020

Akinori Iwai, Fabio Righetti, Benjamin Wang, Osamu Sakai, and Mark A. Cappelli

Physics of Plasmas ARTICLE scitation.org/journal/php

# A tunable double negative device consisting of a plasma array and a negative-permeability metamaterial

Cite as: Phys. Plasmas **27**, 023511 (2020); doi: 10.1063/1.5112077
Submitted: 2 June 2019 · Accepted: 1 January 2020 ·
Published Online: 6 February 2020



Akinori Iwai,[1,2] Fabio Righetti,[2] Benjamin Wang,[2] Osamu Sakai,[3,4] and Mark A. Cappelli[2]

## AFFILIATIONS

[1]Research Institute for Sustainable Humanosphere, Kyoto University, Gokasho, Uji, Kyoto 611-0011, Japan
[2]Stanford Plasma Physics Laboratory, Department of Mechanical Engineering, Stanford University, Stanford, California 94305, USA
[3]Electronic Systems Engineering, The University of Shiga Prefecture, 2500 Hassakacho, Hikone, Shiga 522-8533, Japan
[4]Department of Electronic Science and Engineering, Kyoto University, Kyoto-daigaku Katsura, Nishikyo-ku, Kyoto 615-8510, Japan

## ABSTRACT

Extraordinary wave transmission is demonstrated through a double-negative composite comprised of a negative-permeability array of double split ring resonators and a negative-permittivity array of plasma discharge tubes at microwave frequencies. A transmission peak emerges in a double-negative band and controlling the electron density inside the plasma tubes dynamically regulates the transmission properties. By performing experiments and theoretical calculations, we verify that the composite permits wave propagation with negative permeability and controllable permittivity, which indicates that a tunable negative-refractive-index device is achieved.



Metamaterials are artificially manufactured structures fabricated with small unit cells that behave much like atoms do in bulk materials in their response to electromagnetic (EM) fields. However, unlike naturally occurring materials, metamaterials have the potential to be engineered to have a negative-refractive-index ($N$). The engineering of a negative-refractive-index metamaterial was first demonstrated in the microwave range of the EM spectrum by Smith *et al.*[1] That study used a combination of a metal wire array nested within an array of metallic double-split-ring resonators (DSRRs)—a structure first proposed by Pendry *et al.*[2] A DSRR consists of two concentric C-shape metal rings oriented relative to the EM fields to achieve a negative magnetic permeability ($\mu$) over a small range of frequency spanning a magnetic dipole resonance.[2] Novel negative-index metamaterials were designed for optical frequencies[3,4] after this first demonstration with microwaves.

In many metamaterial designs, a metal wire array is used to make the effective bulk permittivity negative.[1] In regard to its EM response, such an array mimics that of a non-magnetized gaseous plasma[5] because both the wire array and gaseous plasma conform to the same EM field dispersion that results in a relative permittivity $\varepsilon_p(\omega) = 1 - \omega_p^2/\omega(\omega + j\nu)$. Here, $\omega$ is the EM angular frequency, $\omega_p$ is the effective plasma frequency for the wire array, calculated as $\sqrt{2\pi c^2/a^2 \ln(a/r)}$ by Pendry *et al.*,[6] $c$ is the speed of EM waves in a vacuum, $a$ is the spacing between the wires, $r$ is the radius of the wires, and $\nu$ is the EM wave damping frequency due to the wire's finite resistivity. For gaseous plasmas, $\omega_p$ is determined by the electron number density, $n_e$, with $\omega_p = \sqrt{n_e e^2/m_e \varepsilon_0}$, and $\nu$ is the electron-neutral momentum transfer collision frequency. Here, e and $m_e$ represent the electron charge and mass, respectively, and $\varepsilon_0$ is the vacuum permittivity. When $n_e$ is sufficiently high ($\omega < \omega_p$) and damping is sufficiently weak, the plasma has similar EM properties to those of a metal. An incident EM wave experiences imaginary refraction (evanescent field penetration). As a result, plasmas have been used as substitutes for metal in applications such as wave reflectors.[7] The reflection of short-wave radio signals off of the ionosphere is a classic example of the imaginary refractive index properties of naturally occurring plasmas.

The demonstration of photonic crystal behavior in ordered arrays of plasma columns is relatively new. In 2004, Hojo and Mase predicted the existence of a bandgap in a one-dimensional periodic structure consisting of plasmas and dielectric materials.[8] The following year, Sakai *et al.*[9] carried out the first experimental demonstration of the existence of bandgaps in a plasma photonic crystal comprised of a two-dimensional array of plasma discharge columns. Conventional photonic crystals have band gaps defined by the array geometry (lattice constant and column diameters) and the material's constant relative permittivity. However, the plasma photonic crystal can be tuned simply by changing $\varepsilon_p$ (through control of $n_e$). Wang and Cappelli verified

the tunability of the bandgap in a two-dimensional plasma photonic crystal in the microwave range.[10]

Since an array of metal wires can have a similar $\varepsilon_p$ as that of a plasma, we proposed experiments to study the EM response of composites consisting of arrays of DSRRs and an overdense plasma.[11] Recently, we carried out experiments in which the plasma itself is generated by driving the DSRR array to breakdown using high-power microwaves.[12] The interaction between the incident field and composite metamaterial gave rise to second harmonic wave generation which we attributed to the nonlinear coupling between the plasma and the DSRR.[13] Few experiments have been carried out demonstrating compelling evidence of a negative $N$ in such plasma metamaterial composites despite indications from numerical simulations,[14,15] even though plasma metamaterials have attracted particular interest not only for the control of EM waves in the microwave regime, but also at optical frequencies.[16] Kim and Hopwood recently reported wave propagation through composites consisting of electric field-resonant negative-$\mu$ split-ring resonators (SRRs) embedded in an inductively coupled plasma.[17] Recent advances have been made on the possibilities of forming left-handed materials that consist of dielectric resonators, which afford a much lower loss than the metallic split ring counterparts.[18] Navarro *et al.* recently studied microwave propagation through an overdense plasma in which a new type of metallic resonator, a so-called sparce SRR contributing a negative permeability, is immersed.[19] Both of these recent studies used experimental configurations in which the plasma is in close proximity to the SRRs. Below, we report on an experimental demonstration of the negative-$N$ behavior of EM wave propagation in composites consisting of an array of DSRRs and an array of overdense plasma columns. The former serves as a metamaterial with a negative-$\mu$ response, while the latter serves as a metamaterial with a negative-$\varepsilon$.

The DSRRs for this experiment are configured as 35 $\mu$m thick copper (Cu) patterns of concentric split rings [see Fig. 2(a)] on supporting FR4 ($\varepsilon_r \sim 4.2$) substrate plates (150 mm × 200 mm) to obtain a magnetic resonant frequency of approximately 2 GHz. The magnetic resonant frequency can be calculated from the effective capacitance and inductance of the DSRR. The former is estimated from the capacitance between two wires,[20] and the latter is determined using the Neumann method.[25] The DSRRs were fabricated using a wet etching process. The patterns are printed on one side of the FR4 plates and the spacing of the rings in the array as well as the spacing of the plates are 20 mm. A total of 70 DSRRs are patterned on any one plate (10 along the vertical side × 7 along the horizontal side). The surface of the Cu DSSRs is coated with a 40-$\mu$m polyimide film ($\varepsilon_r \sim 3.2$) to prevent a direct contact between the plasma discharge tubes and Cu patterns of the DSRRs. When these DSRR arrays are combined with a plasma array that contributes a negative effective $\varepsilon$, a double-negative metamaterial composite can be achieved with a response over a narrow region of the microwave spectrum.

The overdense plasma is achieved through the use of an array of gas discharge tubes used previously to construct a reconfigurable plasma photonic crystal.[10] This plasma photonic crystal can simulate a plasma medium of slightly lower effective density, $\bar{n}_{eff}$, than the average density, $\bar{n}_e$ of the plasma in any single discharge tube by arranging them to have a sufficiently small lattice spacing in comparison to the incident EM wavelength. The plasma metamaterial composite was achieved by inserting the discharge tubes in the gaps between the DSRRs' plates as illustrated in Fig. 1. The discharge tubes, which are

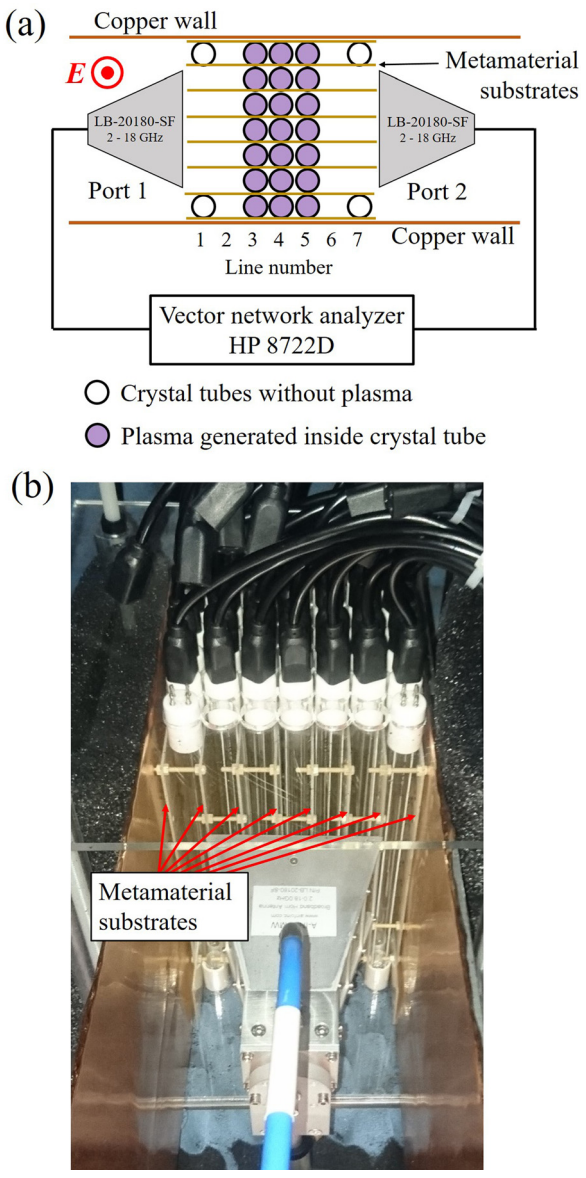


**FIG. 1.** (a) Top view schematic of a composite consisting of a nested array of plasma discharge tubes and DSRRs'. This illustrates a case with plasma tubes on three lines (lines 3, 4, and 5). The electric field radiated from the transmitting antenna is parallel to the tubes. (b) Photograph of the system before plasma generation. Here, 5 lines (lines 2, 3, 4, 5, and 6) are shown occupied with plasma discharge tubes.

290 mm long, 15 mm in outer diameter, and have a 1-mm quartz wall thickness ($\varepsilon_r \sim 3.8$), are arranged in as large as a 7 × 7 square array with a 20-mm spacing in the center and are supported on an acrylic frame. The plasma is formed within the 13 mm inner diameter between an anode and cathode at the top and the bottom of the tube, respectively, and serviced by two Teflon-coated thin copper wires that run parallel to the tubes. The inside of the tube is filled with 250-Pa of argon and a small amount of mercury. We use a variable AC voltage

source that consists of a ballast and a voltage slider to control the peak discharge current, $I_p$, from 25 mA to 111 mA. The gas temperature of the generated plasma inside the tube is approximately 330 K,[21] and is used to estimate the gas density, and, from the discharge voltage, the reduced field strength. As discussed in our previous studies,[10] the reduced field strength is used together with the estimated swarm parameters and the measured discharge currents to obtain estimates of the electron collision frequency and the plasma density.

Two broadband horn antennas (A-Info LB-20180-SF; for 2.0 GHz to 18.0 GHz) are placed in front of (transmitter—port 1) and behind (receiver—port 2) the metamaterial composite to record the transmission (scattering parameter $S_{21}$) with a vector network analyzer (HP 8722D). The polarization is such that the electric and magnetic fields are parallel to the plasma tubes and normal to the plane of the DSRRs, respectively, to obtain the electric response of the plasma array and the magnetic resonance of the DSRRs. Copper walls surround the composite to suppress wave divergence and undesired scattering from the surroundings. We refer to the row of plasma discharges closest to the transmitter as the "1st line" of plasmas, and the line number increases further from the transmitting horn, as shown in Fig. 1. A total of as many as 7 lines can be inserted, and the example illustration in Fig. 1(a) shows plasma tubes inserted on the 3rd, 4th, and 5th lines, which we refer to as the "3-lines" case. In the photograph of 1(b), five lines (2nd -6th lines) are occupied by discharge tubes.

The measured $S_{21}$ spectrum shown in Fig. 2(a) of just the DSRR array (solid black line) is consistent with a medium that experiences a Lorentz-type dispersion with an effective relative permeability

$$\mu_{SReff} = 1 + F\omega_m^2/(\omega_m^2 - j\gamma\omega - \omega^2). \quad (1)$$

Here, $F$ is a constant, $\omega_m$ is the magnetic resonance frequency, and $\gamma$ is the magnetic resonance damping constant.[2] The attenuation arises from the EM impedance mismatch and energy dissipation presented by the array of split rings. The dispersion introduced by the magnetic resonance is seen to result in a peak attenuation of approximately 45 dB centered at ~2.0 GHz. We determine the parameters in the expression for $\mu_{SReff}$ in Eq. (1) as those which best fit the theoretical curve with the experimental $|S_{21}|$ for the metamaterial [Fig. 2(a)], and obtain the parameters $\omega_{m,} = 2\pi \times 2.0$ GHz, $F = 0.5$, and $\gamma = 0.03\omega_m$. With these parameters, the range of negative-$\mu$ is estimated to be 2.0 GHz $< \omega/2\pi <$ 2.47 GHz; this frequency range is highlighted in figures discussing the frequency dependence of wave transmission [e.g., square area in Fig. 2(a)].

The "effective" relative permittivity of the plasma discharge array, $\varepsilon_{peff}$, is estimated using the effective medium theory,[22] which is appropriate when the diameters of the plasma discharges (13 mm) and the plasma spacing (20 mm) are smaller than the incident EM wavelength (~130 mm). In this regards, the plasma photonic crystal acts as a uniform metamaterial of lower overall plasma density. For this analysis, the plasma within the discharge tube is treated as uniform in plasma density with a radius-averaged value of $\bar{n}_e$, even though the actual plasma density is expected to vary across the tube radius. Figure 2(b) shows the variation in $\varepsilon_{peff}$ for different values of $\bar{n}_e$ as determined using the effective medium theory. The value of $\varepsilon_{peff}$ becomes negative in the negative-$\mu$ range of the DSSRs when $\bar{n}_e > 2.0 \times 10^{17}$ m$^{-3}$. We see that $\varepsilon_{peff}$ is positive for average plasma densities $\bar{n}_e < 0.5 \times 10^{17}$ m$^{-3}$. Our previous studies[23] indicate that $\bar{n}_e$ varies from about $0.3 \times 10^{17}$ m$^{-3}$ to $4.0 \times 10^{17}$ m$^{-3}$ over the range in the discharge current, 25 mA $< I_p <$ 111 mA. We see then, that $\varepsilon_{peff}$ is readily varied from positive to negative in this experimental system by changing $I_p$ (applied AC voltage). Figure 3 shows $|S_{21}|$ for a case in which there are two lines of active ($I_d$ = 111 mA) discharge tubes [lines 4 and 5 in Fig. 1(a)] without the presence of any DSRR plates. For comparison, we also show the transmission when the discharge tubes are turned off (black broken line). We see that with the plasma on, there is a cut-off at approximately 6 GHz with the attenuation at about −40 dB in regions where we expect the DSRRs to be active. With the discharge off, the transmission in this range is significantly higher, with an attenuation of at most 10 dB attributed to scattering from the quartz envelopes and lead wires.

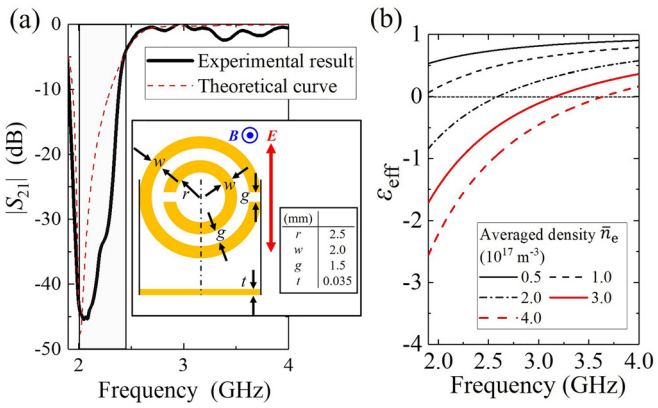


**FIG. 2.** (a) Measured $|S_{21}|$ of the DSRRs' array (no plasma) and theoretical curve calculated by Eq. (1). The square area (2.0 GHz $< \omega/2\pi <$ 2.47 GHz) indicates the estimated negative-$\mu$ region. The DSSR geometry is explained in the inset. (b) Estimated effective relative permittivity of the plasma array tuned by the average density $\bar{n}_e$ of the plasma.

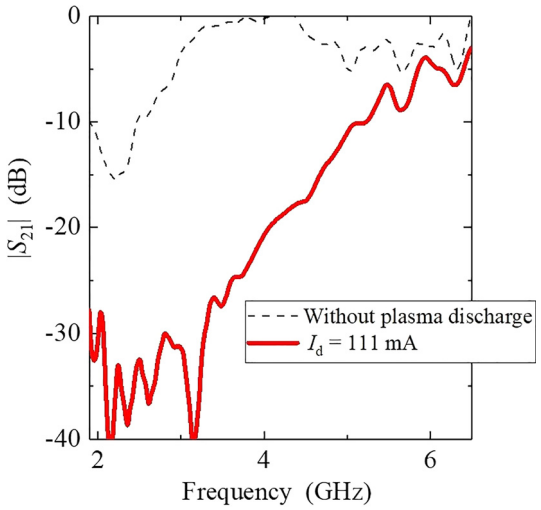


**FIG. 3.** Measured $|S_{21}|$ for 2-lines' of plasma discharge tubes [lines 4 and 5 in Fig. 1(a)] in the absence of DSSR plates without (black broken line) and with an active discharge (red solid line). The discharge current $I_d$ is 111 mA, which is the maximum value used with our discharges.

Here, we focus primarily on the EM response in the vicinity of the double-negative state which satisfies negative-$\mu$ and negative-$\varepsilon$ simultaneously, i.e., the transmission properties of the plasma metamaterial composite from 2.0 GHz to 4.0 GHz. The measured $|S_{21}|$ of the composite for two values of discharge current ($I_p = 25$ mA and 111 mA, corresponding to low- and high-$\bar{n}_e$ cases) and for as many as 5-lines (lines 2–6) of plasma tubes inserted, is shown in Fig. 4. The dashed lines indicate the measured $|S_{21}|$ of just the DSRRs, e.g., Fig. 2(a). According to Fig. 2(b), $\varepsilon_{peff}$ decreases as $\bar{n}_e$ increases, causing reflection from, and absorption in, the plasma array. Where $\mu_{SReff}$ is almost unity ($\omega/2\pi > 2.6$ GHz), the $|S_{21}|$ diminishes with increasing $I_p$ (i.e., higher $\bar{n}_e$ and with increasing number of lines of plasma discharge tubes). When we activate just a single line (line 5) of the plasma tubes, $|S_{21}|$ in the region $\omega/2\pi > 2.4$ GHz for the high $\bar{n}_e$ case is lower than that for the low $\bar{n}_e$ case. However, in the frequency range 2.2 GHz $< \omega/2\pi <$ 2.4 GHz (within the negative-$\mu$ band), we see the opposite response.

Increasing the number of plasma discharge tube lines inserted for the high $\bar{n}_e$ case increases the recovery of $|S_{21}|$ within the negative-$\mu$ range, and a single transmission peak ($|S_{21}| > -30$ dB) is observed as seen in the 5-lines case in Fig. 4. For this case, where $\omega/2\pi > 2.6$ GHz (positive-$\mu$), $|S_{21}|$ is strongly suppressed because the length of the negative-$\varepsilon$ region is greatly extended. For both low and high $\bar{n}_e$ cases, $|S_{21}|$ decreases rapidly under 3.0 GHz also due to the scattering from the small lead wires that run along the length of the tubes. In fact, as we saw in Fig. 3, the $|S_{21}|$ begins to decrease near 3.0 GHz for the case with two inactive lines of plasma tubes indicating that the composite consisting of the DSRRs and plasma discharge tubes actively permits wave transmission when both $\mu$ and $\varepsilon$ are simultaneously negative. This result suggests that this composite achieves a negative-$N$ as demonstrated in previous reports.[1]

Figure 5 depicts the $|S_{21}|$ for the 5-lines case for a range of $I_p$. Again, in the spectral region, $\omega/2\pi > 3$ GHz, decreasing $I_p$ from

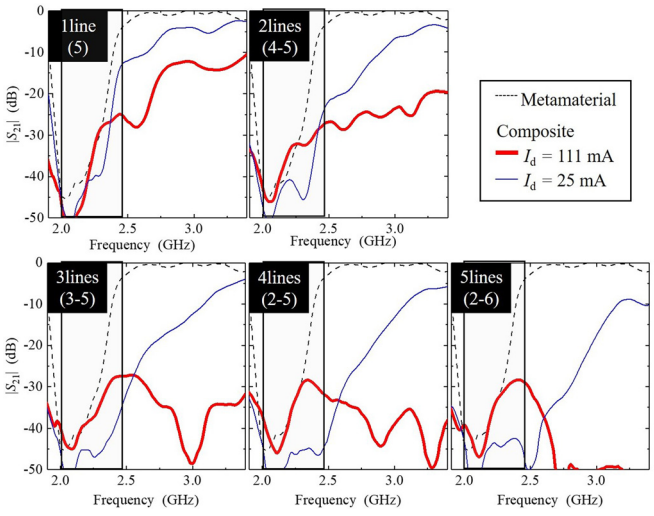


**FIG. 4.** Measured $|S_{21}|$ as a function of frequency for $I_p = 111$ mA and 25 mA and for various plasma lines of tubes inserted into the DSRR array. The values in parentheses indicate the line numbers in Fig. 1. The square area (2.0 GHz $< \omega/2\pi <$ 2.47 GHz) indicates the estimated negative-$\mu$ region.

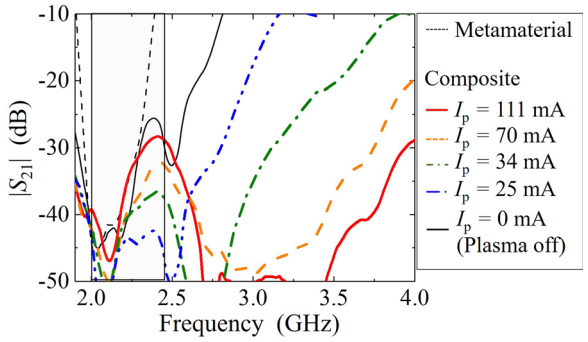


**FIG. 5.** Variation in $|S_{21}|$ by controlling $I_p$ for the 5-lines case in Fig. 4. The square area (2.0 GHz $< \omega/2\pi <$ 2.47 GHz) indicates the estimated negative-$\mu$ region.

111 mA to 25 mA (therefore decreasing $\bar{n}_e$) drastically increases $|S_{21}|$ (by more than 40 dB). This increase is due to the change in $\varepsilon_{peff}$ from strongly negative to positive values in regions where $\mu_{SReff} \sim 1$. However, the behavior is quite different in the negative-$\mu$ range (2.0 GHz $< \omega/2\pi <$ 2.47 GHz), where we see that $|S_{21}|$ increases with increasing $I_p$. For $I_p = 111$ mA, $|S_{21}|$ increases by more than 15 dB beyond that for $I_p = 25$ mA at 2.4 GHz. These results indicate that one can control transmission over a wide frequency range by simply varying $\bar{n}_e$, demonstrating that such a plasma metamaterial composite can be a dynamically tunable device with regions of both positive and negative values of $N$. When $I_p = 0$ mA, $|S_{21}|$ in the negative-$\mu$ range is significantly larger than that for the $I_p = 25$ mA case even though the real part of $\varepsilon_{peff}$ is close to unity because of the electron neutral collisional damping of the EM wave within the plasma tubes.

We have modeled the transmission peak that was observed in the double-negative frequency band for the 5-lines case in Figs. 4 and 5. The $S_{21}$ parameter is determined from the impedance of the plasma metamaterial composite, predicated on the assumption that the $\varepsilon_p$ of the plasma columns and $\mu_{SReff}$ of the DSSRs can be represented with Drude- and Lorentz-type dispersion, respectively. The normalized impedance of the effective medium representing the plasma metamaterial composite, $Z_{eff} = \sqrt{\mu_{SReff}/\varepsilon_{peff}}$, is converted to $S_{21}$ using the relationship between the impedance matrix and the scattering matrix, as described by Pozer.[24] The analysis requires specifying the dispersion parameters that enter into $\varepsilon_p$ and $\mu_{SReff}$ in order to obtain an $S_{21}$ that well represents the one measured. The parameters for $\varepsilon_p$ are guided by our past experiments.[10] In order to reasonably reproduce the $S_{21}$ measured in the negative-$\mu$ band for the composite consisting of the 5-lines of plasma tubes at a discharge current $I_p = 111$ mA, we use the following:

$$\varepsilon_p(\omega) = 1 - \omega_{pe}^2/(\omega^2 + j\nu\omega). \quad (2)$$

Equation (2) is only an approximate expression for the dielectric contribution to the metamaterial composite because the actual composite consists, in addition to the plasma columns, the surrounding quartz envelope and thin metal wires that run along the tube to service the discharge. Furthermore, the plasma has spatial variations in electron density that are not known. As such, these factors may contribute to the collisional damping and plasma density that appear in the equation

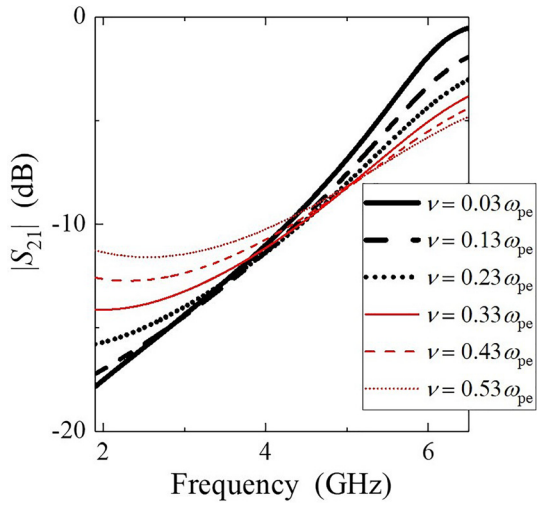


**FIG. 6.** Frequency dependence of $|S_{21}|$ for a 40-mm of dielectric material obeying Eq. (2) and with $\omega_{pe}/2\pi = 5.5$ GHz. The loss parameter $\nu$ varies from 0.03 $\omega_{pe}$ to 0.53 $\omega_{pe}$.

in using this dielectric constant to model the extraordinary propagation in the double-negative frequency band, particularly the frequency-dependence of the amplitude and phase of $|S_{21}|$.

We establish the parameters that enter Eq. (2) by adjusting $\omega_{pe}$ and $\nu$ to obtain reasonable agreement between the modeled and measured $|S_{21}|$ for the 2-line array of plasma tubes (Fig. 3). In particular, we try to capture the high frequency threshold (6.5 GHz) and the location and steepness of the rise of the attenuation feature toward this threshold. We find that values of $\omega_{pe}/2\pi = 5.5$ GHz and $\nu = 0.3\omega_{pe}$ provide reasonable agreement between the predicted and measured $|S_{21}|$ for the 2-line case. The value found for $\omega_{pe}$ is well within the range determined for the same discharge tubes in Ref. 10. The value found for $\nu$ is about a factor of 50% higher, however, it is worth noting that the modeled $|S_{21}|$ is only weakly dependent on the assumed damping rate (see Fig. 6).

Figure 7(a) shows the calculated $|S_{21}|$ for the metamaterial consisting of just the DSRRs (black dashed line, $Z_{eff} = \sqrt{\mu_{SReff}}$) and for the plasma metamaterial composite (red solid line, $Z_{eff} = \sqrt{\mu_{SReff}/\varepsilon_{peff}}$). The assumed length of the effective medium is 80 mm. We find a transmission peak that rises to about −10 dB for the composite in the double-negative region. For $\omega/2\pi > 2.5$ GHz, $|S_{21}|$ decreases to levels of −20 dB. Overall, we see good qualitative and reasonable quantitative agreement with the experiments. Figures 7(b) and 7(c) plot the corresponding $\mu_{SReff}$, $\varepsilon_{peff}$, propagation wavenumber, $k$ for the case without [Fig. 7(b)] and with [Fig. 7(c)] the plasma tubes. In Fig. 7(b), the real part of $k$, Re($k$), rapidly approaches zero maintaining positive values in the negative-$\mu$ range, and the imaginary part of $k$, Im($k$), originates from the losses of the metamaterial, $\gamma$ in Eq. (1). In the case of the plasma-metamaterial composite, Re($k$) has negative values in the negative-$\mu$ range due to negative $\varepsilon_p$, which indicates a negative-index state. In the negative-$\mu$ range, 2.0 GHz $< \omega/2\pi <$ 2.47 GHz, $|S_{21}|$ is similar for the two cases, but $|S_{21}|$ for the composite case never exceeds that of just the metamaterial because of the electric damping of the EM wave modeled by $\nu$ in Eq. (2), which is reflected in Im($k$) in Fig. 7(c). Figures 8(a) and 8(b) show the modeled phase of $S_{21}$, represented as $\theta_{S21}$, for the metamaterial and the composite. It is worth noting that there are stark differences in the phase, $\theta_{S21}$ when comparing the composite to the metamaterial alone. In Fig. 8(a), we see that $\theta_{S21}$ increases only gently with frequency as $k$ approaches a pure imaginary value at around 2.4 GHz [Fig. 7(b)] and an evanescent wave exists in the negative-$\mu$ range. In Fig. 8(b), $\theta_{S21}$ is seen to increase strongly with frequency, passing through zero several times, indicating the presence of a propagating mode in the negative-$\mu$ range as $k$ crosses over from a positive to a negative real value.

According to Fig. 4, the 5-lines case with $I_p = 111$ mA, $|S_{21}|$ for the plasma-metamaterial composite almost matches that for the DSRRs' array in the range 2.2 GHz $< \omega/2\pi <$ 2.4 GHz as reproduced by the model in Fig. 7(a). In Figs. 8(c) and 8(d), we examine the relative behavior of $|S_{21}|$ and $\theta_{S21}$ seen experimentally. For the DSRRs' array only [Fig. 8(c)], $\theta_{S21}$ decreases with increased frequency over the range 2.2 GHz $< \omega/2\pi <$ 2.4 GHz, and then increases for $\omega/2\pi >$ 2.4 GHz. The same behavior is seen in the model [Fig. 8(a)]. In contrast, the plasma-metamaterial composite case [Fig. 8(d)] shows that $\theta_{S21}$ increases over the range 2.2 GHz $< \omega/2\pi <$ 2.4 GHz, consistent with that of [Fig. 8(b)], even though $|S_{21}|$ reaches a maximum. We see that the experimental measurements of both $|S_{21}|$ and $\theta_{S21}$ are in

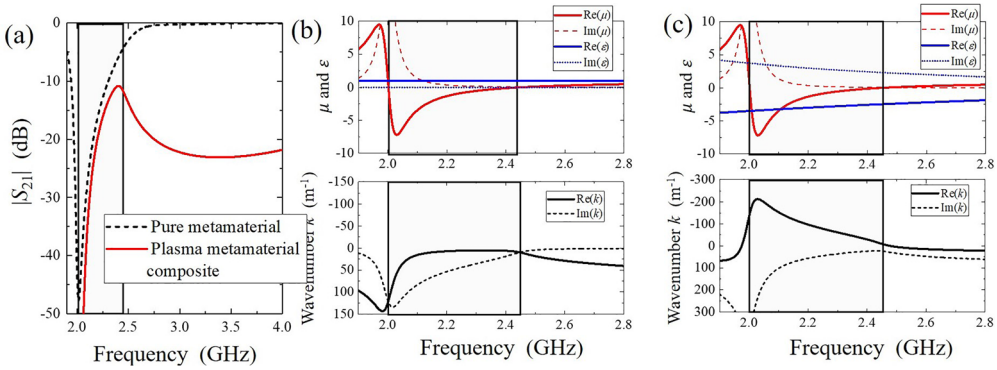


**FIG. 7.** (a) Modeled $|S_{21}|$ for a metamaterial and a plasma-metamaterial composite. Values of $\mu_r$, $\varepsilon_r$, $k$, and $\theta_{S21}$ for (b) a metamaterial and (c) a plasma-metamaterial composite. The square area (2.0 GHz $< \omega/2\pi <$ 2.47 GHz) indicates the estimated negative-$\mu$ region.

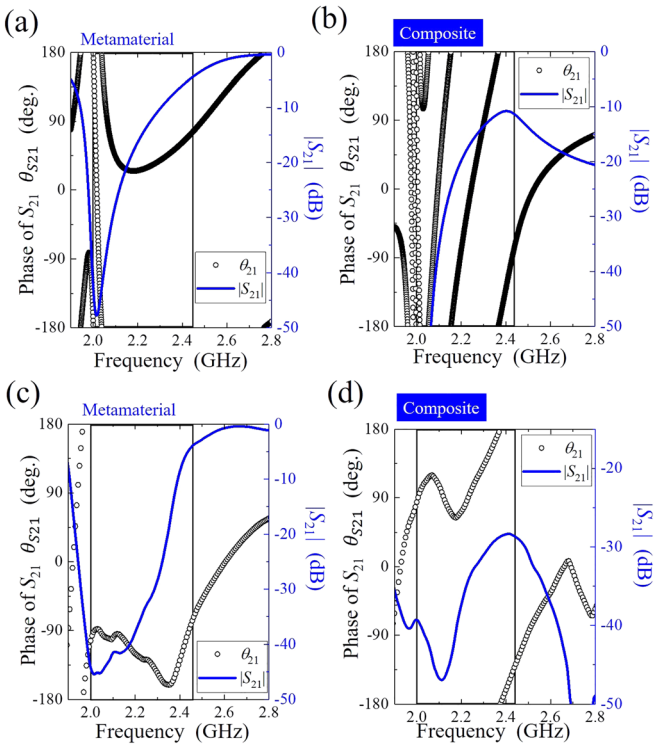


**FIG. 8.** Calculated $\theta_{S21}$ and $|S_{21}|$ for (a) the metamaterial and (b) the composite. Measured $\theta_{S21}$ and $|S_{21}|$ for (c) the DSRRs array and (d) the composite with the 5-lines plasma tubes at $I_p = 111$ mA. The square area ($2.0\,\text{GHz} < \omega/2\pi < 2.47\,\text{GHz}$) indicates the estimated negative-$\mu$ region.

reasonable agreement with the model, which indicates that the plasma-metamaterial composite supports the propagation through a negative-$N$ medium.

This study demonstrates wave propagation through the plasma-metamaterial composite, which consists of an array of plasma discharge tubes and DSRRs, the latter of which had a negative $\mu$ in the range of $2.0\,\text{GHz} < \omega/2\pi < 2.47\,\text{GHz}$. We found a transmission peak in this negative-$\mu$ range. The transmission of the composite was regulated by controlling $I_p$, as $\varepsilon_{peff}$ is determined by $n_e$, which is sensitive to discharge power. A theoretical model for $|S_{21}|$ and $\theta_{S21}$ is presented that captures the general behavior seen in the experiments, in particular, this transmission peak on the high frequency side of the DSRRs' attenuation band. These results strongly suggest that this plasma-metamaterial composite realizes a tunable negative-$N$ device based on the controllable $\varepsilon_p$ of the plasma.

This work was supported in part by a Grant-in-Aid for Scientific Research from the Japanese Ministry of Education, Culture, Sports, Science, and Technology, a Grant-in-Aid for JSPS research Fellow, and the Overseas Challenge Program for Young Researchers in JSPS. The Stanford program is supported by a Multidisciplinary University Research Initiative from the Air Force Office of Scientific Research.

## REFERENCES

[1]D. R. Smith, W. J. Padilla, D. C. Vier, S. C. Nemat-Nasser, and S. Schultz, "Composite medium with simultaneously negative permeability and permittivity," Phys. Rev. Lett. **84**, 4184 (2000).
[2]J. B. Pendry, A. J. Holden, D. J. Robbins, and W. J. Stewart, "Magnetism from conductors and enhanced nonlinear phenomena," IEEE Trans. Microwave Theory Tech. **47**, 2075 (1999).
[3]V. M. Shalaev, W. Cai, U. K. Chettiar, H.-K. Yuan, A. K. Sarychev, V. P. Drachev, and A. V. Kildishev, "Negative index of refraction in optical metamaterials," Opt. Lett. **30**, 3356 (2005).
[4]G. Dolling, C. Enkrich, M. Wegener, C. M. Soukoulis, and S. Linden, "Low-loss negative-index metamaterial at telecommunication wavelengths," Opt. Lett. **31**, 1800 (2006).
[5]W. Rotman, "Plasma simulation by artificial dielectrics and parallel-plate media," IRE Trans. Antennas Propag. **10**, 82 (1962).
[6]J. B. Pendry, A. J. Holden, W. J. Stewart, and I. Youngs, "Extremely low frequency plasmons in metallic mesostructures," Phys. Rev. Lett. **76**, 4773 (1996).
[7]R. J. Vidmar, "On the use of atmospheric pressure plasmas as electromagnetic reflectors and absorbers," IEEE Trans. Plasma Sci. **18**, 733 (1990).
[8]H. Hojo and A. Mase, "Dispersion relation of electromagnetic waves in one-dimensional plasma photonic crystals," J. Plasma Fusion Res. **80**, 89 (2004).
[9]O. Sakai, T. Sakaguchi, and K. Tachibana, "Verification of a plasma photonic crystal for microwaves of millimeter wavelength range using two-dimensional array of columnar microplasmas," Appl. Phys. Lett. **87**, 241505 (2005).
[10]B. Wang and M. A. Cappelli, "A plasma photonic crystal bandgap device," Appl. Phys. Lett. **108**, 161101 (2016).
[11]O. Sakai and K. Tachinaba, "Plasmas as metamaterials: A review," Plasma Sources Sci. Technol. **21**, 013001 (2012).
[12]A. Iwai, Y. Nakamura, and O. Sakai, "Enhanced generation of a second-harmonic wave in a composite of metamaterial and microwave plasma with various permittivities," Phys. Rev. E **92**, 033105 (2015).
[13]A. Iwai, Y. Nakamura, A. Bambina, and O. Sakai, "Experimental observation and model analysis of second-harmonic generation in a plasma-metamaterial composite," Appl. Phys. Express **8**, 056201 (2015).
[14]O. Sakai, "Transition between positive and negative permittivity in field-dependent metamaterial," J. Appl. Phys. **109**, 084914 (2011).
[15]A. Iwai, O. Sakai, and Y. Omura, "One-dimensional particle simulation of wave propagation and generation of second harmonic waves in a composite of plasma and metamaterial," Phys. Plasmas **24**, 122112 (2017).
[16]M. Moradi and A. R. Niknam, "Terahertz Dyakonov surface waves in plasma metamaterials," Opt. Lett. **43**, 519 (2018).
[17]H. Kim and J. Hopwood, "Wave propagation in composites of plasma and metamaterials with negative permittivity and permeability," Sci. Rep. **9**, 3024 (2019).
[18]L. Fantini, S. Dennison, H. Kim, M. Sarkarat, M. Lanagan, and J. Hopwood, "Plasma reconfigurable metamaterial using a 6.5 GHz dielectric resonator array," J. Appl. Phys. **126**, 203301 (2019).
[19]R. Navarro, L. Liard, and J. Sokoloff, "Effects of a low pressure plasma on a negative-permeability metamaterial," J. Appl. Phys. **126**, 163304 (2019).
[20]T. Sakurai and K. Tamaru, "Simple formulas for two- and three-dimensional capacitances," IEEE Trans. Electron Devices **30**, 183 (1983).
[21]C. Kenty, M. a Easley, and B. T. Barnes, "Gas temperatures and elastic losses in low pressure mercury-argon discharges," J. Appl. Phys. **22**, 1006 (1951).
[22]Y. Wu, J. Li, Z. Zhang, and C. T. Chan, "Effective medium theory for magneto-dielectric composites: Beyond the long-wavelength limit," Phys. Rev. B **74**, 085111 (2006).
[23]B. Wang and M. A. Cappelli, "A tunable microwave plasma photonic crystal filter," Appl. Phys. Lett. **107**, 171107 (2015).
[24]D. M. Pozer, *Microwave Engineering* (John-Wiley & Sons, Hoboken, 2011).
[25]T. D. Corrigan, P. W. Kolb, A. B. Sushkov, H. D. Drew, D. C. Schmadel, and R. J. Phaneuf, "Optical plasmonic resonances in split-ring resonator structures: An improved LC model," Opt. Express **16**, 19850 (2008).